

# Elasticity, Entropy, and the Phase Stability of Plutonium

*Albert Migliori, Joseph P. Baiardo, and Timothy W. Darling*

$$F = E - TS$$

Elastic moduli are the material constants that connect stress with strain and are therefore crucial to engineering applications. They also determine the long wavelength vibrational modes, or sound waves, in a solid and therefore play a leading role in determining how thermal energy is distributed among internal vibrations. Because at ambient temperatures and above vibrational excitations contribute most of the entropy (which is determined by the total number of possible configurations), accurate measurement of elastic moduli as a function of temperature can help us compute much of the energy and entropy, and therefore the free energy, in systems at finite temperature, including plutonium. In fact, a considerable effort at Los Alamos over the last decade has led to the development of resonant ultrasound spectroscopy (RUS) for accurate measurements of elastic moduli in polycrystalline and millimeter-sized single crystal samples. We have recently begun to apply that novel technique to the study of plutonium.

In this article, we explain how this empirical approach to determining the free energy provides an important new avenue for understanding the phase stability of plutonium. First principles electronic-structure calculations have given an impressive description of  $\alpha$ -plutonium, the lowest-temperature phase of plutonium, but no one has developed the tools to calculate the higher-temperature phases from first principles. To do so, one needs to include the effects of temperature and entropy. Theorists cannot do that yet. Instead, many of them point to changes in electronic structure as the key to understanding phase changes. They argue that the gradual localization of the itinerant  $f$  electrons causes the transition from one solid phase to the next. In contrast, we emphasize that both energy and the number of configurations (entropy) contribute to the free energy and are of comparable importance in determining the most probable states and, therefore, the observed phase of a

system. This point of view leads us to attempt answering the following question: What controls the most probable and, therefore, the only observable phases of plutonium? We show that we can estimate large parts of the free energy at temperatures above ambient by measuring elastic moduli and that those data will also enable us to catalog the missing parts. In particular, this approach may enable us to figure out whether or not the localization of the  $f$  electrons is a main ingredient in determining phase instability.

Because plutonium is very soft and has a relatively high melting point, we expect its elastic behavior and entropy to play a big role in explaining its nature. The combination of softness and high melting point alone could lead to some very odd behavior and, in fact, may explain the phase changes of plutonium without requiring the dramatic changes in electronic structure now being invoked by theorists.

Given the fundamental importance of elastic properties, it might seem strange that we have little accurate and reliable elasticity information on plutonium. Moreover, the data we have are decidedly unusual. When Moment and Ledbetter (1975) made the first, and so far the only, measurement on a single crystal of gallium-stabilized  $\delta$ -plutonium—1 weight percent (1 wt %) gallium—they showed that the elastic properties were amazingly anisotropic. The very large shear anisotropy in plutonium means that elastic measurements on polycrystalline samples will produce averages of strongly varying quantities, masking the underlying physics. To get at these details, it is important to make as many measurements as possible on single crystals. However, because powerful regulatory and safety issues come to bear when working with plutonium, only very small (a few millimeters in each dimension) gallium-stabilized  $\delta$ -plutonium crystals will likely be grown in the next several years. Fortunately, RUS is perfectly suited to measuring these small crystals. In this

very simple technique, an analysis of the mechanical resonances of a solid object whose shape is known provides the complete elastic tensor. In the last section of this article, we will describe how RUS is being used to remeasure the elastic moduli of plutonium, both in single-crystal and in polycrystalline materials. We also summarize our latest results.

### Statistics, Free Energy, and Phase Stability

The following rapid review of statistics, the laws of large numbers, and the concepts of temperature, entropy, and free energy is designed to explain how a phase with a higher, and therefore less likely, energy can become stable. Because a higher-energy phase has many more configurations than a lower-energy phase—that is, it has more entropy—the higher-energy phase may be the more probable of the two. The climactic point of this section shows that minimizing the free energy is equivalent to finding the most probable phase.

The configuration of a large group of atoms is called a phase, and the study of what happens to large groups of atoms and what phases they exhibit as temperature or pressure is varied has fascinated scientists for many years. It is, of course, a subject strongly pursued today. One key to understanding phase stability relates to the properties of systems composed of very large numbers of identical objects. When the numbers are really large, there is no hope of computing anything exactly. But one can make approximations, and the accuracy of the approximations becomes outstanding. In fact, very precise predictions arise strictly out of the large numbers.

**Statistics.** Let us take a collection of 8 coins, each with a different date. We put the coins in a sack and then remove them, one by one, and place them in a row. The first coin in the row can be

any one of 8; the second, any one of 7, and so on. Thus the total number of possible arrangements, or states, is  $8 \times 7 \times 6 \times 5 \times 4 \times 3 \times 2 \times 1$ , which is called 8! (eight factorial), and its value is 40,320. But because we were careless in placing the coins in a row, some are heads and some are tails. For the 40,320 ways of placing the coins on the table, there are also 40,320 ways of placing all the coins heads up because each coin has a distinct date. However, if we could not read the date (the coins become indistinguishable from each other), things change.

There are far fewer distinguishable states if the objects are indistinguishable ( $256 = 2^8$ , to be exact, heads or tails for each of 8 objects). Of those 256 states, only one is all heads, and only one is all tails. There is also only one state in which the first coin is heads and the rest of the coins are tails. There is only one state in which the first, second, and fifth coins are heads and all the rest are tails, and so on. Each distinguishable state has the same probability of appearing, namely, 1 in 256. But how many states have 1 head and 7 tails? The answer is 8. That is, the head can be in any one of 8 different positions. How about 3 heads and 5 tails? We have 8 choices for the first head, 7 for the second, and 6 for the third. But when we put the first head in position 1 and the second in position 2, we get the same number of heads as when we put the first head in position 2 and the second in position 1. In fact, there are 6 ways of arranging the order of placing 3 coins heads up. Thus, the total number of states with 3 heads is  $(8 \times 7 \times 6)/(3 \times 2 \times 1) = 56$ . From the above reasoning, we construct the bar graph in Figure 1. The most likely occurrence is equal numbers of heads and tails, and the probability of other outcomes slowly drops as we move to either side of the peak probability of 70/256. In general, we see that the number of states  $\Omega(n)$  of a system of  $N$  objects,  $n$  of which are of one equally probable type and  $N - n$  of which are of the other equally probable type, for

which the exact arrangement of the  $n$  objects is unimportant, is

$$\Omega(n) = \frac{N!}{n!(N-n)!} \quad (1)$$

Recalling the binomial expansion, we can also see that

$$\begin{aligned} (a+b)^N &= a^N + Na^{N-1}b \\ &\quad + \frac{N(N-1)a^{N-2}b^2}{2!} + \dots \\ &= \sum_{m=0}^N \frac{a^{(N-m)}b^m N!}{m!(N-m)!} \end{aligned} \quad (2)$$

If  $a = b = 1$ , then

$$(1+1)^N = 2^N = \sum_{m=0}^N \frac{N!}{m!(N-m)!} \quad (3)$$

which is exactly the sum of all the states. For our example in Figure 1, we knew that the sum was 256, a value we reasoned out by knowing that each object had two possible states and that there were 8 objects.

**The Effect of Large Numbers.** If instead of 8 random flips, we took  $N = 10^{22}$  flips, about the number of atoms in a small chunk of matter, then there are  $2^{10^{22}}$  distinguishable states. The most probable result is equal numbers of heads and tails. If we compute the probability of obtaining equal numbers of heads and tails and call it  $P$ , then what outcome has a probability of  $P/2$ ? Using Equation (3), we find that we get about  $10^{11}$  more heads than tails (or vice versa) with a probability of  $P/2$ . In other words, in  $10^{22}$  flips, it would be reasonably likely to get  $10^{11}$  more heads than tails—the error in getting exactly equal numbers of heads and tails is only a hundred billionth of the total number of flips (that is, about  $1/N^{1/2}$  of the total). We also know there is only one state, far from the maximum probability, in which we get  $10^{22}$  heads. Thus, the width of the peak in the probability distribution is  $N^{1/2}$ , and there is not much left outside the peak.

What we learn from all this is that, as the numbers become large, the peak becomes extremely narrow and that all practically useful information is in the peak. It will be very accurate, later on, to approximate the real peak with a very tall rectangular distribution with constant probability over the width of the peak and zero probability elsewhere. These arguments lead to some important rules for systems (visible pieces of matter) in which the number of identical particles is of the order of Avogadro's number ( $6.02 \times 10^{23}$ ).

The first rule for these macroscopic systems is that we can count on all the numbers to be very large. For that reason, what may seem wildly inaccurate approximations will be nearly exact ones. The errors will be of the order of either the square root of a large number (for example, the square root of  $10^{22}$  is  $10^{11}$ , a much smaller number than the original one) or the logarithm of a large number (for example,  $\ln(10^{22}) = 51$ , which is pretty small compared to  $10^{22}$ ).

The next rule is that any accessible state of the system is equally likely, but we see only the most probable ones. Accessible states are those that do not violate any constraints, such as fixed volume, or physical laws, such as conservation of energy, momentum, or charge. As time passes, a system composed of a large number of objects with a “reasonably large” total energy (we will beg off on the definition of reasonably large for now) explores all the possible arrangements of those objects (each arrangement is a state) near that energy.<sup>1</sup> That is, if we were to take suitably fast snapshots of the system, each picture would be of an accessible state. In more concrete terms, we take our sack of coins, empty it on the floor, count the number of heads, and then repeat the process. But our sack has  $10^{22}$  coins, and we perform the experiment, say,  $10^{11}$  times per second (that is about the number of times per second that a gas molecule undergoes a collision).

<sup>1</sup>There are, however, some systems that violate this ergodicity hypothesis.

sion with another gas molecule).

Because each state is equally likely, we only see very few of the approximately  $2^{10^{22}}$  total possible states. Let us say that the universe will last  $10^{110}$  seconds. Then, in the life of the universe, we will perform the experiment  $10^{121} = 2^{402}$  times. If the experiment is really done on a container of gas instead of a sack of coins, then one possible observable to use instead of the number of heads is the fraction of gas molecules in, say, the left half of the container. The probability of any one atom of gas to be in the left half is  $1/2$ . The probability that all of them are in the left half is  $2^{-10^{22}}$ . The number of times that we observe this configuration to happen in the entire life of the universe is  $2^{-10^{22}} \times 2^{402} \approx 2^{-10^{22}}$ . Therefore, we will not see it happen! What we do see in the time we have to observe it is that the gas mostly accesses the states near the most probable one. That is, the states we see most often are the ones with nearly exactly half the mass in the left side of the container, and the typical variation in that value is  $1/(10^{22})^{1/2}$ , or about 1 part in  $10^{11}$ . In more practical terms, we would expect the measured value of pressure, energy, or other macroscopic physical quantity to be within about 1 part in  $10^{11}$  of its most likely value. The statistical properties of systems of very large numbers come round again to behaving like those of systems of only one or two particles. That is, even though we can only take a probabilistic view of a system that is way too complicated to compute exactly, the results are, for all practical purposes, exact!

The last rule is that the total number of states of a system is a very strongly increasing function of the total energy. We use a simple quantum harmonic oscillator to illustrate this property. Unlike most other physics problems, the statistical mechanics of quantum systems is easier to work with than that of classical systems because the quantum numbers make the counting of states easy. A quantum oscillator might be composed of a mass and spring or

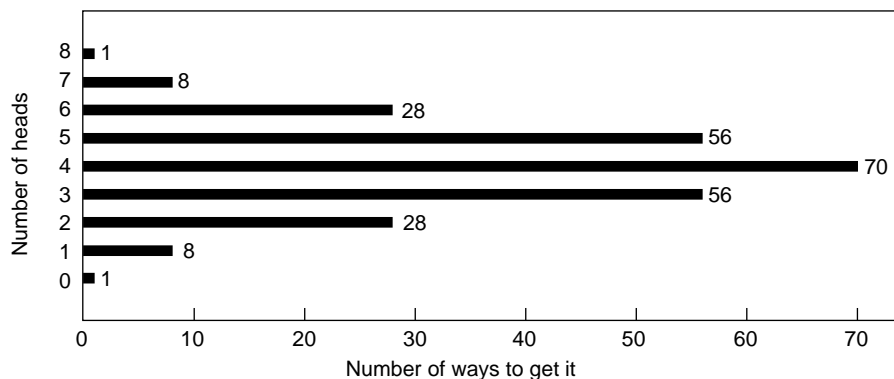


**Figure 1. Number of Heads vs Ways to Get That Number**

This graph shows the number of states of a system of 8 coins in which the only quantity of interest is the number of heads. That is, the 8 coins are indistinguishable, and the order in which a given number of heads is obtained is irrelevant. If we keep track of which toss produced what value, the total number of distinguishable states is 256, the most probable state has 4 heads (and 4 tails), the total number of ways to make that state is 70, and therefore the probability of that state is  $70/256$ .

an atom and a chemical bond. In either case, the energy of the quantum oscillator increases in proportion to the square of the amplitude of vibration. No matter what the amplitude might be, the frequency remains  $f = \omega/2\pi$ , just like the frequency of a tuning fork. The total energy of the oscillator is always  $E = (n + 1/2)\hbar\omega$ , where  $n$  is any positive integer,  $\hbar$  is Planck's constant, and each quantum of vibrational energy is  $\hbar\omega$ . We now consider a set of three harmonic oscillators, as shown in Figure 2. If the total energy of the three oscillators is  $E = (2 + 1/2)\hbar\omega$ , then the system contains two quanta, and it can be in one of six equally probable states (110 means the first oscillator has one quantum, the second has one, and the third has none). The six states are the following:

200 020 002 110 101 011.

If there are three quanta in the system,  $E = (3 + 1/2)\hbar\omega$ . The 10 available states are

300 030 003 210 201  
120 102 012 021 111.

If we increase the energy of the

system, the number of available states increases, as does the average energy of each oscillator, and the increase per oscillator is roughly proportional to the fractional energy increase. Therefore, if we have  $10^{22}$  oscillators, or vibrational modes, as in a solid of  $10^{22}$  atoms, and the total energy of the system is increased by 10 percent, then so is the average energy of each oscillator. Therefore, the total number of states in the systems increases by a factor of  $(1.1)^{10^{22}}$ , or approximately  $2^{1.4 \times 10^{21}}$ , which is an enormous increase. It is now apparent that a reasonably large amount of energy in a system with a large number of objects is enough energy so that roughly every object in that system has more than its ground-state energy.

**Entropy and Temperature.** We will use simple properties of probabilities to generate a universal definition of temperature. Consider a very small chunk of matter that is touching or is part of a very much larger chunk. We assume the total energy of the whole system is fixed at  $E$ ; the smaller piece has an energy  $E_1$ , and the larger has an energy  $E - E_1$ . What is the probability that we observe this configuration? If the number of states of the smaller

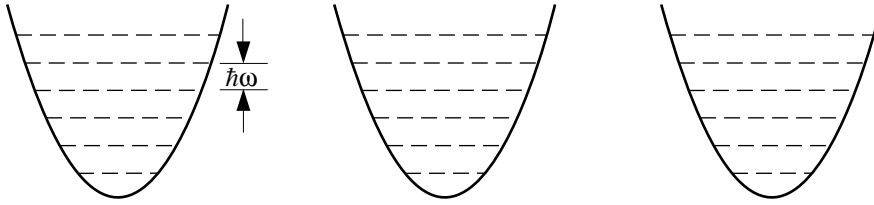


**Figure 2. A System of Three Independent Quantum Harmonic Oscillators**  
 The figure shows the parabolic potential wells and the energy levels (dashed lines) for a system of three independent quantum harmonic oscillators. The energy levels are equally spaced at intervals of  $\hbar\omega$ , where  $\omega$  is the angular frequency of oscillation. That is, we excite the system by adding vibrational energy in quantized units called phonons, and the energy of each phonon is  $\hbar\omega$ . Because the oscillators are indistinguishable, any state of  $n$  quanta is equally likely—no matter how those phonons are distributed among the oscillators. As a result, the average energy per oscillator will be  $n/3$ . Also, the larger the number of quanta, the larger the number of ways to distribute them, and therefore, the larger the entropy of the system.

system is  $\Omega_1(E_1)$  and of the larger system,  $\Omega_2(E - E_1)$ , then the probability of observing this configuration is the product of the probabilities of observing each system separately, and

$$P(E_1) \propto \Omega_1(E_1) \Omega_2(E - E_1) . \quad (4)$$

Note that we have also used the property that the probability of a state of energy  $E_1$  is proportional to the total number of states with energy  $E_1$ . To convert Equation (4) to an equality, we must divide it by the total number of states  $\Omega_{\text{total}}$ . To find this constant, we must first compute the total number of states for each value of  $E_1$ , where  $E_1$  ranges from zero to  $E$ , and then add up those numbers.

Equation (4) is a very important result. Let us therefore review what it means. Things in each system are whizzing and banging around all the time. Considered individually, the systems do not have fixed energy, and therefore the number of states of each system will vary as energy is exchanged between them. Every time we look at the whole system, we will see it in one of its equally likely configurations. We have shown that, as energy increases, the number of states increases very rapidly. Conversely, if energy

decreases, the number of states drops very rapidly. Because the large and small subsystems are in thermal contact, they trade probabilities. Equation (4) is a very sharply peaked function that is the product of a rapidly increasing function of  $E_1$  and a rapidly decreasing function of  $E_1$ . For large numbers, the maximum is extremely sharp—in fact, so sharp that it is unlikely that anything but the most probable configurations will ever be observed. Thus, after a while, no matter what the initial states were, the system is observed near its most likely configurations (those that are near the maximum in the probability distribution). Those configurations divide the energy between the two subsystems in a very special way: The fractional increase in the number of configurations of the smaller system, as energy is added to it, is exactly matched by the fractional decrease in the number of configurations of the larger system, as energy is removed from it. That is, for small fluctuations in the energy of either part of the system, the overall probability stays about the same, or

$$\frac{dP(E_1)}{dE_1} = 0 = \Omega_2 \frac{d\Omega_1}{dE_1} - \Omega_1 \frac{d\Omega_2}{dE_1} . \quad (5a)$$

Using the properties of the natural logarithm, this expression becomes

$$\frac{d \ln \Omega_1}{dE_1} = \frac{d \ln \Omega_2}{d(E - E_1)} . \quad (5b)$$

Equation (5b) expresses one property common to both systems once they have reached thermal equilibrium, something we already know about. What we know is that, after a while, the temperature of both systems is the same. The definition of the temperature is

$$T = \left( k_B \frac{d \ln \Omega}{dE} \right)^{-1} , \quad (6)$$

where  $k_B$  is Boltzmann's constant. We also define entropy to be

$$S = k_B \ln \Omega . \quad (7)$$

The definition of entropy is particularly important because it represents a general way for constructing an additive quantity from multiplied probabilities. From Equations (4)–(7), we see that thermal equilibrium occurs when the temperatures of the subsystems are the same, which is equivalent to saying that the system is very near a maximum probable configuration. We also see that, because the logarithms of products add, entropy is a good extrinsic quantity (2 pounds of butter have twice the entropy of 1 pound).

The system will, however, also exhibit a strange property relating to entropy. We already mentioned the intuitively attractive property that no matter in what state we start the system, after a while, it will be observed in one of its very probable accessible configurations (mathematically equivalent to maximum entropy). All the physical laws apparently governing this system are time reversal invariant. Therefore, if we go either forward or backward in time, entropy should increase. Whenever we observe this system, its entropy must be a mini-

num—something the universe does not, in fact, provide for. If the system was in a very probable configuration in the past, it will continue to be in a very probable configuration in the future.

But if it was in a very improbable configuration in the past, the system will rapidly adjust itself to a probable configuration. The behavior of entropy is not time reversal invariant (we cannot tell the state of the system in the past by observing it in the present). To quote the English translation of “Statistical Physics” by L. D. Landau and E. M. Lifshitz (1980),

“The question of the physical foundations of the law of monotonic increase in entropy thus remains open: it may be of cosmological origin and related to the general problem of initial conditions in cosmology; the violation of symmetry under time reversal in some weak interactions between elementary particles may play some part. The answers to such questions may be achieved only in the course of further synthesis of physical theories.”

**Free Energy.** To make the connection between statistics and quantities we can measure, we need to study how to calculate the values of measurables if we know the probabilities of possible states. Consider a small system in exactly one definite state  $i$  of energy  $E_i$  (there are many states with energy  $E_i$ ) connected to a much larger system of energy  $E - E_i$ . Then a simple Taylor expansion yields

$$\ln \Omega(E - E_i) \cong \ln \Omega(E) - \frac{d \ln \Omega}{dE} E_i, \quad (8)$$

or

$$\frac{\Omega(E - E_i)}{\Omega(E)} = e^{-\frac{E_i}{k_B T}}, \quad (8)$$

where we used the definition of temperature and relied on  $E_i$  to be small. We can easily compute probabilities from

Equation (8) by remembering that the sum of all the probabilities is 1. The correct normalized probability, where the sum is over each distinct state  $i$ , is

$$P_i = \frac{e^{-\frac{E_i}{k_B T}}}{\sum_i e^{-\frac{E_i}{k_B T}}}, \quad (9)$$

which describes the probability of observing a state  $i$  with energy  $E_i$ . The numerator of Equation (9) is the famous Boltzmann factor. The equally famous partition function is the normalization factor in Equation (9), with one term for each allowed state of energy  $E_i$  such that

$$Z = \sum_i e^{-\frac{E_i}{k_B T}}. \quad (10)$$

There are, however, many states  $\Omega(E_i)$  with energy near  $E_i$ . Equation (10) can therefore be rewritten as a sum over each distinct energy  $E_i$ , and we will find that

$$Z = \sum_{E_i} \Omega(E_i) e^{-\frac{E_i}{k_B T}}. \quad (11)$$

Because numbers are large and probability distributions sharply peaked, we can accurately approximate the real shape of  $\Omega(E_i)$  by a rectangular distribution that is constant over the approximate width of the real distribution and zero everywhere else. The width and height are adjusted so that the area of the rectangle is the correct total number of states near the energy. “Near” in this case can be very crude, and errors in it and this process will only affect the answers to the order of  $\ln \Omega$ , which is an extremely small error. With these approximations, we perform the sum in Equation (11) to obtain

$$Z \cong \Omega(\bar{E}) e^{-\frac{\bar{E}}{k_B T}} = e^{-\frac{F}{k_B T}}, \quad (12a)$$

where  $\Omega(\bar{E})$  is the total number of states near the most probable energy and  $F$  is the free energy. Because

$$\ln Z = \ln \Omega(\bar{E}) - \frac{\bar{E}}{k_B T}, \quad (12b)$$

we can express the partition function solely in terms of the free energy and temperature:

$$-k_B T \ln Z = \bar{E} - TS = F. \quad (12c)$$

The significance of writing the partition function in this way is as follows. If the system can be in two phases at once (ice in water), somehow, the fantastically large numbers and wildly swinging probabilities must conspire to make both phases equally likely, even though their energies are obviously different. In addition, the partition function  $Z$  must now have two pieces, one for ice and one for water. For the two phases to be observable simultaneously, keeping in mind the monstrous numbers, the two pieces of the partition function must be equal. Therefore, we see that, when the free energy of ice per molecule equals the free energy of water per molecule, the partition functions for equal numbers of molecules are equal, or

$$\begin{aligned} Z_{\text{water}} &= \Omega_{\text{water}}(\bar{E}_{\text{water}}) e^{-\frac{\bar{E}_{\text{water}}}{k_B T}} \\ &= Z_{\text{ice}} = \Omega_{\text{ice}}(\bar{E}_{\text{ice}}) e^{-\frac{\bar{E}_{\text{ice}}}{k_B T}}. \end{aligned} \quad (13)$$

The number of molecules and, therefore, the number of accessible states are typically so large that, if the free energies of the two phases differ, only the phase with the lowest free energy is sufficiently probable to be observed. This is the primary concept that determines the observed phase.

Note that the likelihood of observing a state with a particular energy is equal to the product of (1) the number of states with that energy and (2) the probability of observing any one of them.

Thus, both the energy and the entropy control the phase stability. In the example of ice and water, the increase in energy per molecule associated with stretching and breaking the bonds that lock water into a frozen state makes water less probable by itself because of the Boltzmann factor. But because there are many more ways to arrange the molecules in the liquid than in the solid, this reduction in probability is offset by the increase in the number of states of water. When the energy is just right, the overall probabilities (free energies) of each phase are equal, and ice begins to melt.

## Phase Stability and Plutonium

We have seen how both the energy and entropy contribute to determining the free energy and therefore the most probable states (phases) of a system. We will now consider the various contributions to the phase stability of plutonium.

At low temperature and pressure, the monoclinic  $\alpha$ -phase of plutonium is stable. This phase is predicted by minimizing the internal energy associated with the electronic structure. In fact, modern electronic-structure calculations by John Wills and coworkers appear to describe completely and astonishingly accurately the behavior of the low-temperature phase of plutonium, essentially from first principles. These calculations are performed for the system at zero temperature, and thus entropy, or the number of states available, is neglected because the entropy contribution to the free energy is zero at zero temperature. It is interesting that plutonium retains the zero-temperature phase to about 400 kelvins, and the electronic-structure calculations predict well the behavior throughout this temperature range.

As temperature rises, the theorist must decide how to include the effects of temperature in determining the free energy. In addition to the internal electronic energy, the contributions to the free energy include a harmonic vibra-

tional (phonon) piece, a thermally activated conduction electron piece, and as Duane C. Wallace writes (1998), an aggregate piece associated with anharmonic phonons and electron-phonon coupling. Of these, the harmonic phonon contribution to the entropy is by far the largest, whereas the aggregate and electronic pieces are less than 6–12 percent of the total. Still, the anharmonic terms give rise to important effects, including thermal expansion, and cause the phonon frequencies (which, in turn, affect the entropy and specific heat) to be temperature dependent. It is attractive, therefore, to use all the available data to attempt to understand the harmonic phonons as perhaps the largest contributor to the root causes of the unusual set of structures that plutonium exhibits.

We will consider first the electronic structure. Remember that isolated atoms in a vacuum have completely localized unmovable electrons with no overlap between the electronic wave functions of different atoms. As the atoms move closer together, the wave functions of their valence electrons overlap weakly at first. The electrons are now shared among the atoms and contribute to the bonding that holds the solid together, but they are hard to move (effectively heavy) from one atom to the next. As the overlap increases, the electrons in a metal become more and more mobile and finally may behave as a gas of nearly free electrons as they do in sodium. For metals such as plutonium, in which the 5f electrons have little overlap, it is not surprising that the crystal structure is very open (otherwise more overlap would occur) and that the overlap and hence the degree of localization are extremely sensitive to interatomic spacing and therefore to pressure. Such a system is expected to be very compressible. As a result, vibrational motion should increase more than usual with increasing temperature as should anharmonic effects so that the average atomic separation should also increase, producing a greater variety of phases than in a system in which overlap is

already strong. Note that the thermal-expansion coefficient of iron is about 13 parts per million per kelvin (ppm/K) whereas that for  $\alpha$ -plutonium is near 42 ppm/K.

To get an idea of the extreme compressibility of plutonium, the bulk modulus (an elastic constant describing the stiffness against hydrostatic compression) of  $\alpha$ -plutonium that we have measured on high-quality research samples is about 55 gigapascals. In contrast, the bulk modulus of ordinary steel is about 170 gigapascals. The stiffest phase of plutonium is therefore three times easier to compress than steel!

Increasing the temperature does not only cause thermal expansion, but it also increases the entropy. Associated with this increase is the selection of high-entropy/high-energy phases that become more and more favorable as temperature rises. Wallace (1998) provides a very careful computation of the total entropy of plutonium as a function of temperature (and phase) by using the best currently available specific-heat data. He finds that by far the largest contribution to the entropy of plutonium at temperatures above ambient is that from the harmonic vibrations. To get an idea of the energy scales,  $TS$  for  $\delta$ -plutonium at the  $\delta$ - $\epsilon$  phase boundary is about 735 milli-electron-volt (meV) per atom, whereas the enthalpy change ( $\Delta TS$ ) between the  $\delta$ - and  $\epsilon$ -phase is on the order of 20 meV per atom. Thus, the  $\delta$ -phase differs from the  $\epsilon$ -phase by only 20 meV per atom, which is a very small fraction of the free energy and is tough for the theorist to compute accurately.

**Vibrational Entropy and Elastic Constants.** Here we show how the vibrational entropy of plutonium can be estimated from measurements of elastic constants, or sound speeds. We begin by approximating plutonium as a collection of masses and springs. This mass/spring, or harmonic, picture connects directly to such mechanical properties as the Young's and shear

moduli, compressibility, and speed of sound, all critical quantities for the best-known practical application of plutonium-239. Consider a long, thin bar of plutonium of length  $L$  (we will keep it under a kilogram or so, just to be safe). If we set the bar to vibrating, the lowest tone, or normal mode, is the one whose half-wavelength just fits in the bar,  $\lambda/2 = L$ . (That wavelength is very much longer than the springs connecting the atoms—therefore, the system behaves as if it were continuous). For the next higher tone, two half-wavelengths fit in the bar; for the next, three fit; and in general,  $n\lambda/2 = L$ , where  $n$  is an integer. In a perfect simple cubic crystal of  $N$  atoms, there are  $N$  allowed tones, or wavelengths, for a given type of vibrational mode, and there are three types of modes—one compressional and two shear. We have a total of  $3N$  normal modes. Each tone (mode) has a fixed frequency but can have any amplitude (careful there, with plutonium, anyway). Thus, each mode is just like the simple harmonic oscillator discussed above. For the lower-frequency normal modes, the frequency  $f$  is  $f = nv_S/(2L)$ . In this expression,  $v_S$  is a sound speed (compressional or different types of shear speeds), and  $n$  is an integer less than about  $N^{1/3}$ , which is about the number of atoms in a row along the length  $L$  of the bar. From all this, it is apparent that the sound speeds control the lower frequencies of the vibrations in plutonium.

To compute the vibrational contribution to the entropy at temperatures above 300 kelvins, we need to find all the vibrational modes, even those higher-frequency modes whose wavelengths are comparable to the atomic spacing. Neutron scattering measurements can, in principle, measure them all (rather imprecisely and with great difficulty), but we can make very good guesses if we know the sound speeds to high accuracy, and even better guesses if we can use sound speed data to constrain approximate data from neutron scattering methods. Ultrasonic techniques, even the ones we employ, determine

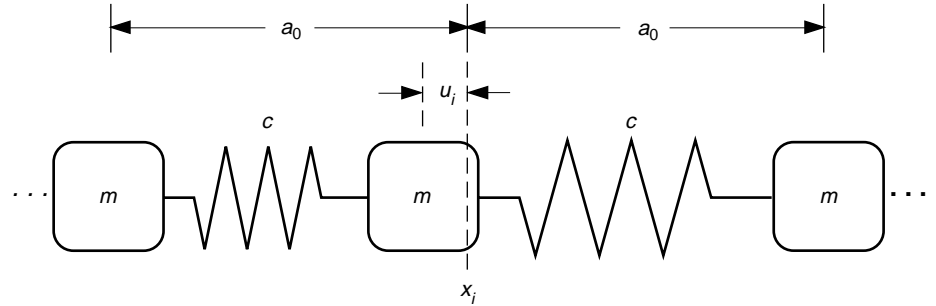


**Figure 3. Elastic Forces in the Harmonic Picture of a Solid**

In the harmonic picture of a solid, a very long string of atoms connected by chemical bonds and separated by  $a_0$ , the lattice constant, or interatomic distance, is represented as a very long string of masses  $m$  connected by springs. The strength of those springs is measured by the elastic constant  $c$ . The distance  $u_i$  is the displacement of each mass from its rest position  $x_i$ , and Equation (14) in the text describes the elastic forces that result from displacements that stretch and compress the springs. The wavelike solutions to Equation (14) describe the longitudinal sound waves that will propagate in this idealized harmonic solid.

the sound speeds only at very long wavelengths, but once we measure the long wavelength modes, with a little help, we can make a pretty good estimate of the variation of frequency with wavelength from our harmonic picture of the solid.

We imagine a very long string of  $N$  masses (atoms), each at a distance  $a$  from its nearest neighbors, and each connected to those neighbors by springs (bonds) as shown in Figure 3. Looking at one of the masses at position  $u_i$ , we find that the stretching of springs to the left and right of that mass produces an acceleration (Newton's famous  $F = ma$ ) such that

$$n \frac{d^2 u_i}{dt^2} = -c(u_i - u_{i-1}) + c(u_{i+1} - u_i). \quad (14)$$

We can solve Equation (14) to find the relationship between the allowed wavelengths and the vibrational frequencies. For each allowed wave vector  $k = 2\pi/\lambda$ , there is a solution with angular frequency  $\omega = 2\pi f$ ,

$$u_i(t) = u_{i0} e^{i(kx_i - \omega t)}, \quad (15a)$$

where the relationship between  $k$  and  $\omega$  (also called the dispersion relation) is given by

$$\omega = \sqrt{\frac{2c}{m}} \sin ka. \quad (15b)$$

The shortest wavelength  $\lambda$  must be greater than twice the interatomic spacing, or  $2a_0$  (if any shorter, we could describe the wave as if it had a longer wavelength and get exactly the same motions), and an integral number of half wavelengths must fit along the string,  $n\lambda/2 = L$ . In other words,  $k = n\pi/Na_0$ , and the largest value of  $k$  is  $\pi/a_0$ . Thus, there is a discrete set of allowed wave vectors, and the frequencies given by Equation (15b) define a discrete set of vibrational modes.

The plot of these discrete vibrational modes versus wave vector in Figure 4 looks continuous because the number of modes is very large. The slope of the straight line, which is the slope of the curve at the origin, is typically the sound velocity and is given by  $d\omega/dk = v_S = a_0(2c/m)^{1/2}$ , where  $c$  is the elastic constant in Equation (14). It is important to note that this simple picture is for nearest-neighbor springs only. As is also shown in the figure, second-nearest neighbors change things, but still the curves are tightly constrained. Our measurements of sound speeds (or elastic constants) are essentially within only a few parts per million away from zero in Figure 4. The flattening of the curve

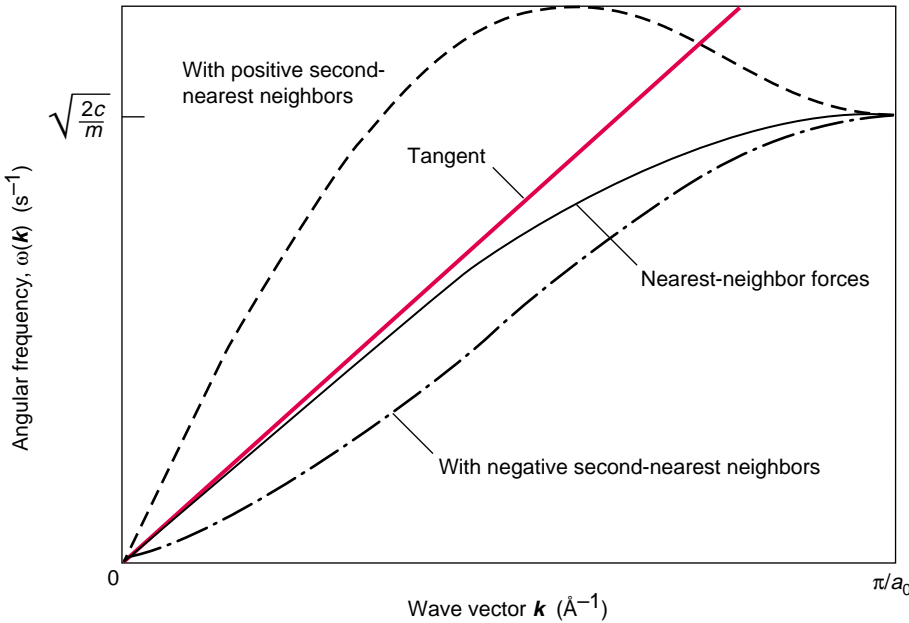


**Figure 4. Vibrational Modes vs Wave Vector**

The black solid curve is a plot of Equation (15b), the dispersion relation (or frequency versus wave vector) for the longitudinal sound-wave solutions to Equation (14). That equation describes forces (springs) between nearest neighbors only. The slope of that curve at  $k = 0$ , marked by the red straight-line tangent, is the sound velocity,  $v_s = a_0 (2cm)^{1/2}$ . The dispersion curves for systems that have either positive or negative second-nearest neighbor forces (in addition to nearest-neighbor forces) are also shown.

at high wave vectors (short wavelengths) is the effect of the discrete system over the continuous one.

For the real solid, the plot is four-dimensional, with three dimensions for the directions of the wave vector and one dimension for frequency. The end-point of the plot in any direction depends on details of the crystal symmetry. In addition, there are three branches in each direction, two for the shearlike waves and one for the longitudinal wave (see Figure 5). The shear-wave speeds are usually about two-thirds of the longitudinal-wave speed. For plutonium and body-centered-cubic (bcc) metals, some shear-wave speeds are much lower. Therefore, the shear modes have lower frequencies of vibration and contribute more to the entropy as we shall see next. Note that in a real solid, the elastic constant  $c$  generalizes to a fourth-rank elastic-modulus tensor with as many as 21 independent elements.

But because most plutonium samples currently available are isotropic polycrystalline samples, much of the directional information is lost, and we can measure only two elastic moduli:  $c_{11}$ , the compressional modulus, and  $c_{44}$ , the shear modulus. In general, each elastic constant is the ratio of a particular type of stress to a particular strain.

Interestingly, if we knew all the sound speeds (or elastic moduli), we could have a good guess at the full four-dimensional plot of the vibrational modes (the phonon dispersion curve) because the frequency dependence is always expected to be very close to that given by Equation (15b) or one of its next-nearest-neighbor analogues. Even in systems with more than nearest-neighbor forces, the general forms of the dispersion curves are tightly constrained, with only a few parameters needed to describe them.

Once the frequency of an oscillator is known, it is very easy to compute its

entropy directly from the partition function—Equation (10). We mentioned earlier that the energy levels of each harmonic oscillator or normal vibrational mode  $i$  are equally spaced, that is,  $E_i = (n+1/2)\hbar\omega_i$ . The average number of quanta (phonons) thermally populating that mode can be written as

$$\begin{aligned} \bar{n}_i &= \frac{1}{Z} \sum_{n=0}^{\infty} n e^{-(n+1/2) \frac{\hbar\omega_i}{k_B T}} \\ &= \frac{1}{\frac{\hbar\omega_i}{k_B T} - 1}, \end{aligned} \quad (16a)$$

where we have used the partition function to compute the expectation value of the number of phonons in that mode. Note that, if the temperature (or  $k_B T$ ) is high relative to the energy of each phonon, there is a simple expression for the average number of phonons in that mode:

$$\bar{n}_i \approx \frac{k_B T}{\hbar\omega_i} \quad \text{for } k_B T \gg \hbar\omega_i. \quad (16b)$$

Based on the result for the average occupation number of mode  $i$ , we can obtain expressions for the average energy in that mode,  $\bar{E}_i$ , and the free energy  $F_i$ :

$$\bar{E}_i = \hbar\omega_i \left( \bar{n}_i + \frac{1}{2} \right) = k_B T, \quad (17)$$

$$F_i = -k_B T \ln Z, \quad (18)$$

where

$$Z = \frac{1}{e^{\frac{\hbar\omega_i}{2k_B T}} - e^{-\frac{\hbar\omega_i}{2k_B T}}}.$$

The entropic contribution to the free energy for a single mode  $TS_i$  is

$$TS_i = \bar{E}_i - F_i. \quad (19a)$$

If the temperature is relatively high, that is,  $k_B T$  is much greater than the energy per phonon, the entropic

contribution in (19a) becomes

$$TS_i \approx k_B T (1 + \ln \bar{n}_i). \quad (19b)$$

We want to know the vibrational entropy of the entire system, and so we need to compute an average over all modes  $i$  of the  $\ln \bar{n}_i$ , or, at relatively high temperatures, an average of  $\ln \hbar \omega_i$ . The Debye temperature, or more exactly,  $k_B \Theta_D$  is a special low-temperature average of  $\hbar \omega_i$  rather than an average of the  $\ln \hbar \omega_i$ . A better characteristic temperature in the high-temperature limit could be computed by taking an average over Equation (19b) for all the modes along all the dispersion curves in a four-dimensional plot. If we define this temperature in the high-temperature limit to be  $\Theta_0$ , then the total vibrational contribution to the entropic term in the free energy is

$$TS \approx 3Nk_B T \left(1 + \ln \left(\frac{T}{\Theta_0}\right)\right). \quad (20)$$

With Equation (20), we have arrived at a description of the total vibrational entropy of a solid of  $N$  atoms, and we have shown that it can be calculated from a measurement of the speed of sound at all wavelengths and in all directions. Measured sound speeds can also be compared with those computed directly from theoretical models of plutonium energy. Therefore, sound speeds or, equivalently, elastic moduli are important for determining both the entropy and energy contributions to the free energy. It is for this reason that measurements of the elastic modulus tensor, dependent on the type of strain and its direction, provide so much stronger feedback to the theorist than simple scalar thermodynamic measurements such as heat capacity or bulk modulus. Surprisingly, only a few sound speeds are known for plutonium, and these are mostly averages obtained from measurements on polycrystalline samples. At present, there is only one measurement at ambient temperature of the full elastic-modulus tensor on a gallium-stabilized  $\delta$ -plutonium single crystal.

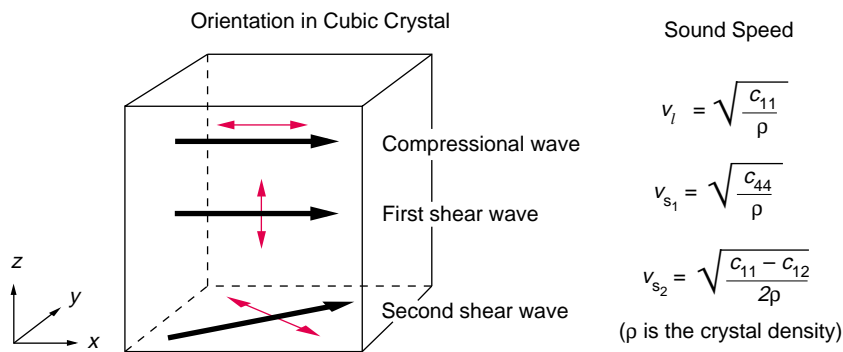


**Figure 5. Vibrational Modes and Sound Speeds in a Cubic Crystal**

There are three types of sound waves. One is a longitudinal wave in which atoms vibrate (red arrow) along the direction of propagation (black arrow), and two are shear waves in which the atoms vibrate perpendicular to the direction of propagation. In a cubic crystal, these waves are associated with three independent elastic moduli— $c_{11}$ ,  $c_{12}$ , and  $c_{44}$ . As shown in the figure,  $c_{11}$  determines the speed of the longitudinal wave,  $c_{44}$  determines the speed of the first shear wave, and  $c_{11}$  and  $c_{12}$  determine the speed of the second shear wave.

#### Estimated Free-Energy Changes and the Role of Entropy in Stabilizing Plutonium

Because the elastic constants in plutonium are very low, we expect the average number of quanta in each mode, and therefore the vibrational entropy, to be high in the high-temperature phases of plutonium. We would even guess that vibrational entropy could be the primary ingredient in stabilizing all the phases of plutonium with the exception of the  $\alpha$ -phase. It would be nice if the changes in entropy and electronic energy in going from phase to phase could be computed from first principles, but it is extremely difficult to compute the electronic energy with the atoms vibrating. Instead, we suggest that one can estimate large parts of the free energy on either side of a phase boundary by measuring elastic moduli and that those data will also enable identification of the missing contributions—especially any changes in the zero-temperature internal electronic energy in going from the  $\alpha$ -phase to the higher-temperature phases. In particular, this approach may enable us to figure out the magnitude of the contribution played by

f-electron localization in determining phase stability in plutonium.

**The  $\delta$ - to  $\epsilon$ -Phase Transition.** We will estimate changes in contributions to the free energy across plutonium's  $\delta$ - to  $\epsilon$ -phase transition at 753 kelvins. This face-centered-cubic (fcc) to bcc transition follows a Bain's path (discussed later) and is most likely to be explained by vibrational- and/or elastic-entropy arguments. There is no net change in free energy across a phase boundary, so any change in internal vibrational (elastic) and electronic energy must be balanced by a change in entropy. One obvious change in the internal energy in going from the  $\delta$ - to  $\epsilon$ -phase is triggered by volume changes. A crude guess for this contribution can be based on the measured bulk modulus  $B$  of  $\delta$ -plutonium (measured, of course, by the sound speeds as well as by x-ray diffraction). Suppose we precompress plutonium isothermally just below this phase boundary by 3.58 percent, the measured volume decrease across the boundary (plutonium shrinks in volume on warming throughout the range of existence of the  $\delta$ -phase and also upon transition to the  $\epsilon$ -phase). We will wind up with a state at the correct volume

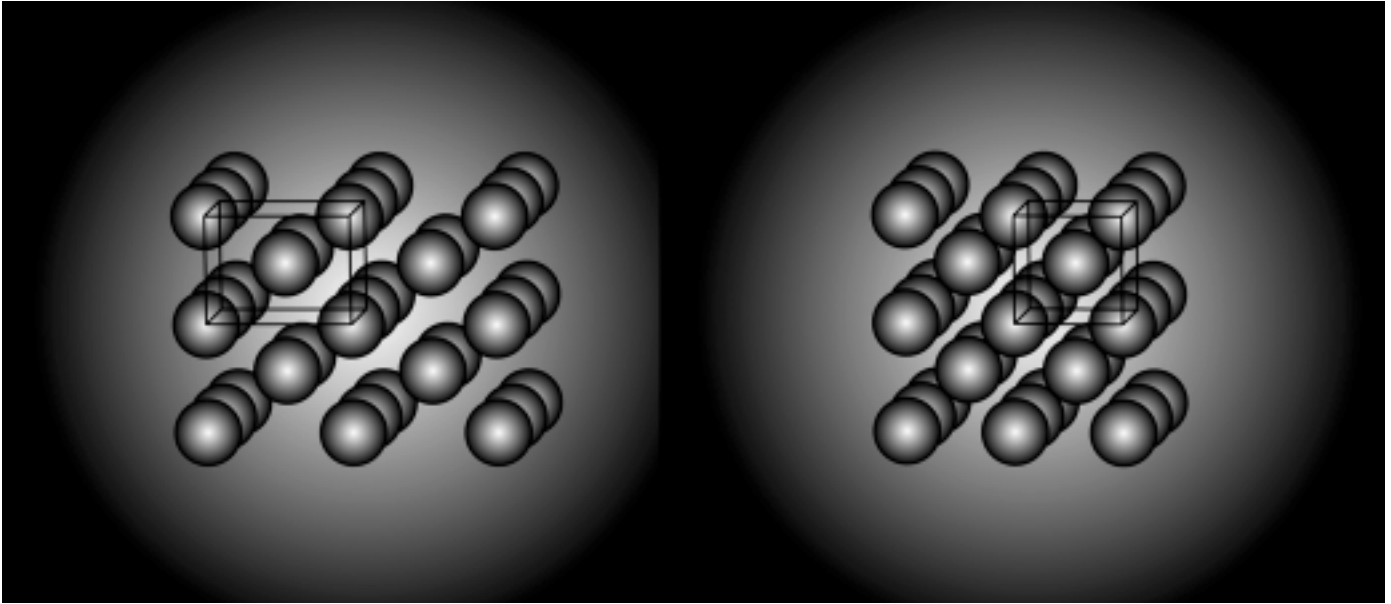


**Figure 6. The Bain's Path for the  $\delta$ - to  $\epsilon$ -Phase Transition in Plutonium**

The figure on the left shows the fcc structure of  $\delta$ -Pu, and the one on the right the bcc structure of  $\epsilon$ -Pu. The particular viewing angle and the unit cell outlined on the left show that the fcc phase is equivalent to a bct phase in which the long edge is  $2^{1/2}$  times the short edges of the unit cell. From this view of the fcc phase, it is clear how the system can shrink continuously from the fcc to the bcc structure. That path is called a Bain's path.

for the  $\epsilon$ -phase but at a temperature infinitesimally too low for it to be stable and having the wrong structure. The compressional energy to make this state is

$$\Delta\bar{E} = \frac{1}{2} B \left( \frac{\Delta V}{V} \right)^2. \quad (21)$$

Using the unit cell size of  $\delta$ -plutonium, four atoms in 4.64 cubic angstroms, and the bulk modulus  $B = 29$  gigapascals,<sup>2</sup> we find that the energy required to compress is 3 meV per atom. The measured latent heat for the  $\delta$ - to  $\epsilon$ -phase transition is about 20 meV per atom. So, simply changing the volume of plutonium cannot account for the internal-energy change. We also learn that elastic moduli other than the bulk modulus must be controlling this transition, and therefore,

<sup>2</sup>This value comes from our recent very accurate RUS measurements on polycrystals, and it agrees well with the only single-crystal elastic-modulus measurements of gallium-stabilized  $\delta$ -plutonium.

simple scalar quantities such as specific heat will not provide all the information we need.

If the volume change does not explain the 20 meV per atom of latent heat, where should we look? We note that, at 753 kelvins, the thermal energy per atom is  $3k_B T = 192$  meV per atom, an enormous energy. It is therefore very attractive to see if much of the latent heat goes into vibrational entropy, which is then balanced by increases in vibrational (elastic) energy, thereby ensuring a zero change in free energy across the transition.

$$\Delta E = T\Delta S. \quad (22)$$

If we can get most of the latent heat with vibrational entropy alone via sound speed changes across the phase boundary, perhaps only small changes in electronic structure are needed.

Figure 6 suggests the type of strain or distortion that could eat up 20 meV per atom. On the left is the fcc  $\delta$ -plutonium structure, shown as the

exactly equivalent bct structure with the long edge  $2^{1/2}$  times larger than the short edges. If we are at a temperature just below the  $\delta$ - $\epsilon$  phase boundary and we uniaxially and isothermally stress  $\delta$ -plutonium so that it shrinks from fcc to bcc (it shrinks along the stress direction and expands perpendicular to it), we produce a bcc structure at just below the temperature at which it is stable. This is a Bain's path. On raising the temperature a tiny amount, absolutely nothing happens except that the bcc structure becomes stable. There is no latent heat for this final step. Therefore, the measured latent heat without a Bain's strain must be equal to the energy required to strain the fcc phase into a bcc shape along the Bain's path. A small volume adjustment might be needed, but we have shown this to be a small effect. What strains are involved in this process?

Measured elastic properties of  $\delta$ -plutonium show an unusually large shear anisotropy. The shear stiffness in

one direction (110, or an angle  $\pi/4$  from an edge) is very low compared to the shear stiffness parallel to an edge. For that reason, Young's modulus, exactly the modulus encountered along the Bain's path, is also very low. Also, Poisson's ratio, which describes how much a material bulges when uniaxially compressed, is very large (0.424, a value close to Poisson's ratio for a liquid). Hence, the Bain's path is traversed with little volume change, and the energy required goes mostly into shear strain energy. We have now connected a change in shear strain energy to the measured latent heat, and we learn that shearlike rearrangement of the plutonium atoms must be the important process at this phase transition! Can we get a handle on this argument via sound speeds as well?

In general, bcc materials have a very large shear anisotropy, typically even larger than for  $\delta$ -plutonium. We expect, then, that the generally low shear stiffness in one direction of bcc structures should provide those modes with lots of entropy, thereby making the bcc structure favorable as the temperature rises. From standard ultrasound measurements by Ledbetter and Moment (1975) and Kmetko and Hill (1976), we obtain the low-temperature average phonon frequencies, or Debye temperatures (not the right average, but at least related to what we want), for both  $\delta$ - and  $\epsilon$ -plutonium. Those characteristic temperatures are 106 kelvins for  $\delta$ -plutonium and 89 kelvins for  $\epsilon$ -plutonium. Using those not-quite-right characteristic temperatures to compute the entropic contribution to the free energy at 750 kelvins—Equation (20)—we find that the measured latent heat  $Q$  balances the change in vibrational entropy perhaps to within 10 percent. In other words,

$$\begin{aligned} 3k_{\text{B}}T \left( 1 + \ln \left( \frac{T}{\Theta_{\delta}} \right) \right) + Q \\ = 3k_{\text{B}}T \left( 1 + \ln \left( \frac{T}{\Theta_{\epsilon}} \right) \right). \quad (23) \end{aligned}$$

Thus, we can account for essentially all the energy and entropy changes in the  $\delta$ - to  $\epsilon$ -phase transition from sound speed (elastic constant) changes. Do these changes in elastic moduli come strictly from the typical changes that occur when a material goes from fcc, a phase expected to have low shear anisotropy, to bcc, a phase expected to have high shear anisotropy, or are the modulus changes a result of changes in electronic structure? Although much more work must be done to establish the relevance of these arguments for the lower-temperature phases, for which the entropy is less, an approach based on ultrasound studies appears the right route to understanding the higher-temperature phases.

The Bain's path may account for the negative volume thermal-expansion coefficient of  $\delta$ -plutonium as well. The very large strains that accompany the Bain's route ensure that, using the latent heat and the starting and ending moduli, we can only roughly construct the elastic moduli along the route. There is also no constraint that the end-point volume be larger or smaller than the starting volume. For plutonium, the end-point bcc volume just happens to be smaller, and the route is very soft—that is, the value of Young's modulus is low along the Bain's path. Therefore, an attractive argument for the negative thermal expansion coefficient of the volume is that, at temperatures below the boundary between the  $\delta$ - and  $\epsilon$ -phase, plutonium thermally "samples" the bcc volume along the very soft Bain's path. Thus, part of the time, it has a volume closer to bcc, which is smaller than the fcc volume. The negative thermal-expansion coefficient of the volume may be a direct consequence of the lower bcc volume and the existence of a Bain's path.

The size of these entropy-driven effects is very large in plutonium. For example, in nickel, which has a melting point almost twice that of plutonium, the bulk modulus is about five times higher, and the Debye tem-

perature (related to the sound speeds and therefore the bulk modulus) is four times higher than in plutonium. Therefore in nickel, compressional energies are larger than in plutonium, and entropy effects are smaller. Nickel has far fewer options in its search for stable high-temperature phases. It also exhibits far fewer structures than plutonium over the range of existence of the solid and always has a positive thermal-expansion coefficient. We might guess then that the root of plutonium's odd behavior may be the localized electrons with weak overlap that force plutonium to have an easily compressed open structure.

## Elastic Moduli Measurements

By now we have probably convinced the reader that knowing the elastic modulus tensor as a function of temperature and pressure for each of the phases of plutonium would be required for a complete experimental understanding of its thermodynamics. Although such data exist for many elements, we have only sparse data for plutonium. To determine the complete elastic tensor using ultrasonic techniques, we must have single crystals of each phase. The phase changes plutonium undergoes as it cools from the melt hinder us from growing single crystals of  $\alpha$ -plutonium unless the metal is under extreme pressure. All the other phases exist only at high temperature. Thus, a single crystal of pure  $\delta$ -plutonium would have to be kept at above 550 kelvins for the entire measurement process. Moreover, because plutonium-239 absorbs neutrons, neutron scattering studies must use pure plutonium-242, and that is a rare isotope. Finally, measuring the moduli in such a dangerous system requires extreme environmental and safety overhead. All these factors combined result in little accurate and reliable elasticity and thermodynamic information on plutonium.

**Implications of Previous Data.** The few data we have, as stated above, are decidedly unusual. Table I shows a summary of the only existing elastic data measured from a plutonium single crystal. These measurements were made by Moment and Ledbetter (1975) at ambient temperature on a 7-millimeter-long  $\delta$ -plutonium grain stabilized with 3.3 atomic percent (at. %) gallium. It took them over a decade to find suitable methods for growing measurable single crystals of plutonium. Their results show that  $\delta$ -plutonium is amazingly anisotropic. Note that  $c^*$  is the shear modulus at an angle of  $\pi/4$  to the cubic axis,  $c_{11}$  controls the longitudinal sound speed, and  $c^*$  and  $c_{44}$  control shear speeds.

Several points must be made about this measurement. First, at a radioactive heating rate of 50 milliwatts per cubic centimeter ( $\text{mW}/\text{cm}^3$ ), larger crystals cannot be measured accurately because they heat internally as a result of their larger surface-to-volume ratio. Second, gallium-stabilized  $\delta$ -plutonium is different from pure  $\delta$ -plutonium. That is, in a crystal of plutonium stabilized with 3.3 at. % gallium, there are only about two plutonium atoms between each gallium atom along any of the principal crystallographic directions. Thus, the presence of gallium thoroughly distorts the structure, the phase transitions, the temperature at which the transitions occur, and even the sign of the thermal-expansion coefficient. Although the atomic volume of the plutonium-gallium (PuGa) alloy varies very smoothly with decreasing gallium concentration and intercepts the atomic volume of pure  $\delta$ -plutonium as the gallium content goes to zero, the elastic properties are often more than an order of magnitude more sensitive to atomic volume than other physical quantities. Thus, it is possible that the elastic moduli of pure  $\delta$ -plutonium are different from those of gallium-stabilized  $\delta$ -plutonium. Third, the elastic anisotropy  $c_{44}/c^*$  is the largest for any fcc metal. (An isotropic system, such as glass, has  $c^* = c_{44}$ .) This strong variation of mod-

**Table I. The Elastic Moduli of  $\delta$ -Pu (1 wt % Ga) at Ambient Temperature<sup>a</sup>**

Modulus	Measured Value (GPa)
$c_{11}$	$36.28 \pm 0.36$
$c_{44}$	$33.59 \pm 0.11$
$1/2(c_{11} - c_{12}) = c^*$	$4.78 \pm 0.38$

<sup>a</sup>Results are from measurements by Moment and Ledbetter.

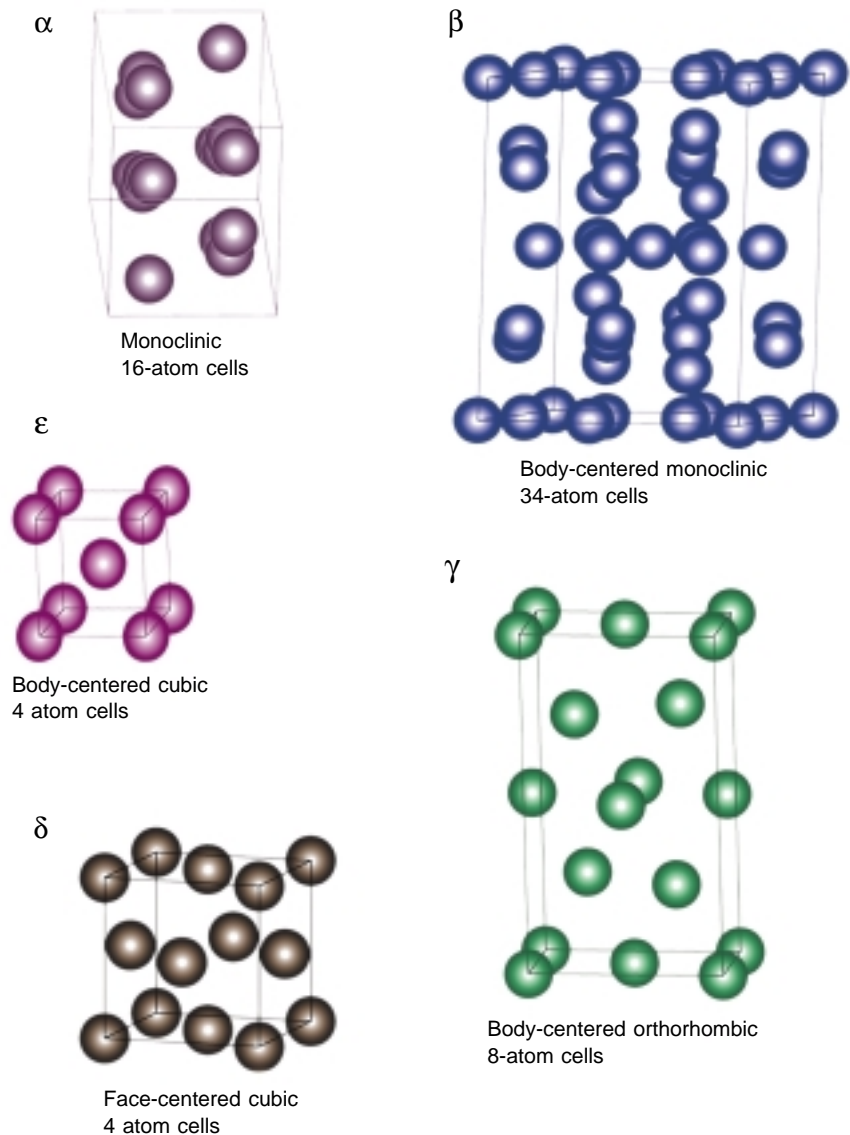


**Figure 7. The Six Crystal Structures of Plutonium**

Starting from  $\alpha$ -Pu and proceeding clockwise are five of the six crystal structures of plutonium in the order in which they appear as the metal is heated. The sixth structure,  $\delta'$  (which occurs between  $\delta$ - and  $\epsilon$ -phase), is not shown because  $\delta'$  and  $\delta$  look about the same.

uli with direction means that we must take more care when computing averages, especially because the soft directions contribute more strongly to entropy. Fourth,  $c_{44}$  nearly equals  $c_{11}$ , and therefore the material does not change volume much when compressed along a cubic axis; in other words, it acts a lot like a liquid. Fifth, radiation damage changes the properties of plutonium. Taken together, these comments suggest that modulus data derived from PuGa alloys are not necessarily applicable to pure  $\delta$ -plutonium and that elasticity measurements must be made to determine the effect of gallium. Nevertheless, we can work with the gallium-stabilized phases, which are crucial for engineering applications. As a result, our initial measurements were focused on those materials.

Finally, we note that, because of the very large shear anisotropy in plutonium, elastic measurements on polycrystalline samples will produce averages of strongly varying quantities, masking the underlying physics. To get at these details, we must make as many measurements as possible on single crystals. That information is necessary to check electronic-structure calculations and develop a fundamental understanding of plutonium. Figure 7 shows the crystal structures of five of plutonium's six solid phases (the  $\delta'$ -phase, which looks like a slightly compressed version of the fcc  $\delta$ -phase, is not shown). The cubic phases have only three independent elastic moduli whereas the monoclinic phases have 13 such moduli.

### Resonant Ultrasound Spectroscopy.

The powerful regulatory and safety issues that come to bear will likely allow only gallium-stabilized  $\delta$ -plutonium crystals of a few millimeters to be grown in the next several years. But small samples are difficult to study with conventional pulsed ultrasound because of both size and attenuation effects. Fortunately, RUS<sup>3</sup> is perfectly suited for remeasuring plutonium's elastic moduli in both single-crystal

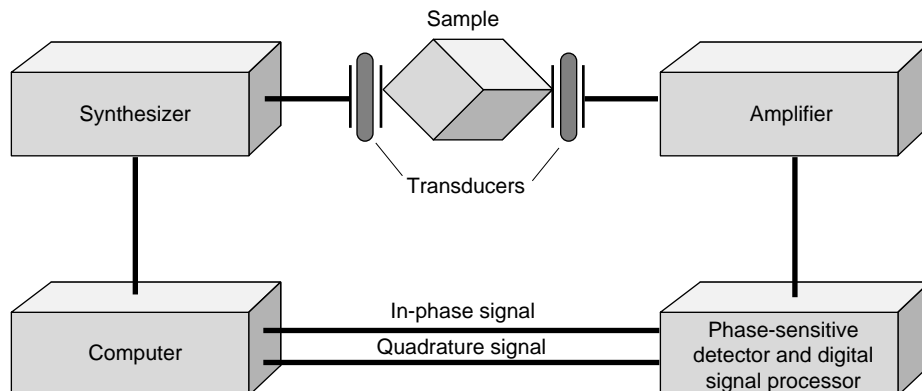


**Figure 8. Block Diagram and Photo of a Resonant Ultrasound Spectrometer**

The resonant ultrasound spectrometer measures a sample (shaped as a rectangular parallelepiped), which is placed between two transducers, one of which drives the sample over a continuous range of frequencies in the megahertz range. While the temperature is held fixed, an electronic-signal generator (or synthesizer) changes the frequency of the driver gradually and automatically. The applied signal is amplified when it passes through regions where the sample resonates. The amplified signal is picked up by the second transducer and recorded automatically by a specially designed electronic phase-sensitive detector. The requisite resonance spectrum at a given temperature is measured in several seconds and is displayed on the computer. Most important, the computer calculates the elastic constants.

and polycrystalline samples.

RUS is a very simple technique, in which the mechanical resonances of a solid object of known shape are induced, measured, and analyzed to provide the complete elastic tensor. This technique is usually implemented on a sample with all faces either parallel or perpendicular to each other (a rectangular parallelepiped resonator, or RPR). Because weak, dry point contact

is made between transducers and very small samples (a few millimeters or less on one side), this system is both extremely accurate and well suited for glove-box operations. The weak contact requires that extreme care be taken with the electronics. Figure 8 shows a block diagram of the current state-of-the-art system.<sup>4</sup> Figure 9 shows the very sharp resonances observed with this system when a typical sample is measured.

<sup>3</sup>Resonant ultrasound spectroscopy (RUS) was developed into a practical tool by Albert Migliori at Los Alamos over the last several years.

<sup>4</sup>The current system was designed by Albert Migliori and is manufactured by Dynamic Resonance Systems, Inc.

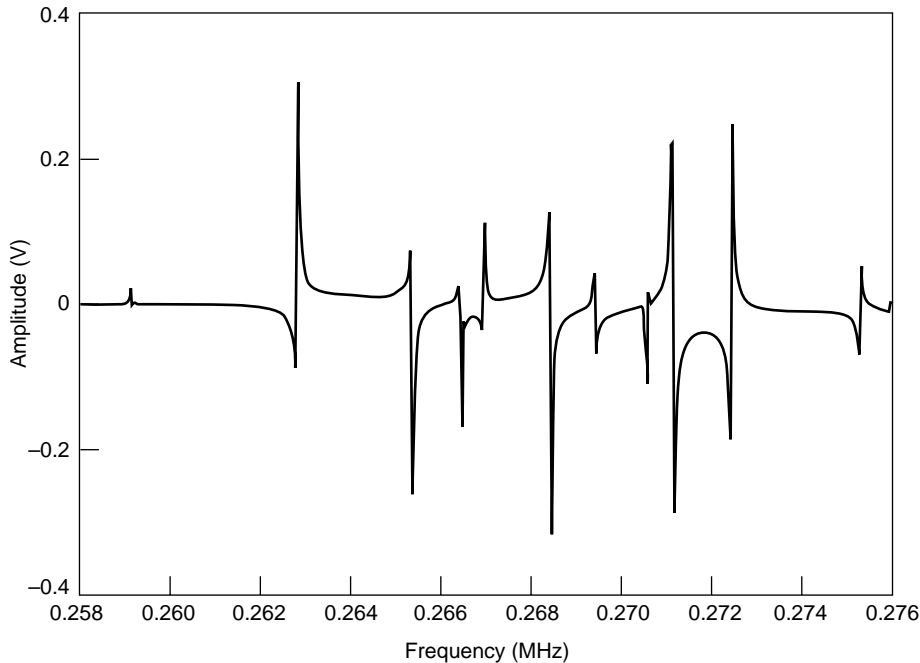


**Figure 9. RUS-Measured Resonances of a High-Purity Plutonium Sample**  
 This spectrum of resonant vibrational frequencies of a high-purity polycrystalline sample of Pu 3.3 at. % Ga was recently measured by our resonant ultrasound spectrometer, which was adapted for use in a glove box environment. Because the resonant ultrasound measurement is phase sensitive, some peaks are negative.

These data were obtained from a high-purity chill-cast new polycrystalline sample of plutonium with 3.3 at. % gallium supplied by Jason Lashley. (See the article “Preparing Single Crystals of Gallium-Stabilized Plutonium” on page 226.) The measure of sharpness of a resonance, or  $Q$ , is  $f/\Delta f$ , where  $f$  is the frequency of a resonance and  $\Delta f$  is the full width at half maximum of the resonance. For our plutonium samples,  $f$  is about 0.2 megahertz. If  $Q$ , which is a direct measure of the intrinsic dissipation, is greater than 1000, we expect very high accuracy for elastic-modulus measurements. For plutonium, we observe  $Q$ s greater than 10,000.

Although acquiring extremely accurate resonances on carefully prepared plutonium samples is straightforward, analysis of those resonances is computationally intensive. To put this statement in perspective, a computation

took 1 second of CPU time on the first Cray, 12 hours on a PC-AT, and now 1.3 seconds on a 600-megahertz Pentium III. In Figure 10, we show the complex deformations corresponding to several particular mode types. These deformations need to be calculated. The RUS algorithm must iteratively compute the deformations and then adjust the elastic moduli of the model RPR to match the measured ones. A typical result is illustrated in Figure 11, showing the deviation between fitted and measured resonances. The actual accuracy of the measurement is not quite the root-mean-square error in the fit because the best fit has different curvatures in the different directions of elastic-modulus space. Typically, we obtain shear moduli on plutonium to better than 0.1 percent and compressional moduli to better than 0.7 percent. Because there are no corrections to such results, RUS typically provides the

highest absolute accuracy for any routine modulus-measurement technique. For the measurement of Figure 11, we used a sample weighing 1.33 grams, with a geometrically determined density of 15.968 grams per cubic centimeter ( $\text{g/cm}^3$ ). The sample was rather large for RUS measurements,  $0.3081 \times 0.4928 \times 0.5603$  centimeters. The errors for this measurement were about 0.9 percent for  $c_{11}$ , which determines the compressional-wave speed, and 0.1 percent for  $c_{44}$ , which determines the shear wave speed.

In Table II, we provide a summary of both our recent measurements and previous measurements by others. Of particular interest is the almost exact correspondence between the very careful measurements of Moment and Ledbetter on a single crystal of new plutonium (3.3 at. % gallium) and our measurement on a nominally identical polycrystal sample. Other measurements, however, unexpectedly disagree. For example, the data for the 3.2 at. % gallium sample are very different. The reason may be an uncontrolled variable (age) or the data may simply be wrong. Moreover, our modern measurement of pure polycrystalline plutonium ( $\alpha$ -phase) at room temperature agrees with one older measurement but not with the other. Finally, the variation in the results of pure plutonium in the  $\delta$ -phase at higher temperatures is so extreme that those results beg for corroboration. We hope to address all these points and others in the next few years.

For all the measurements we have made on plutonium, the  $Q$ s were greater than 3000 and as much as 12,000 for the sample whose data are illustrated in Figure 11. With a  $Q$  of 10,000 and signal-to-noise ratios typified by Figure 9, we are able to track frequency changes smaller than 1 ppm. This extraordinary sensitivity to changes makes possible two unique measurements. The first is done in real time and is a measurement of the effect of radioactive decay on the elastic properties of plutonium. For example,

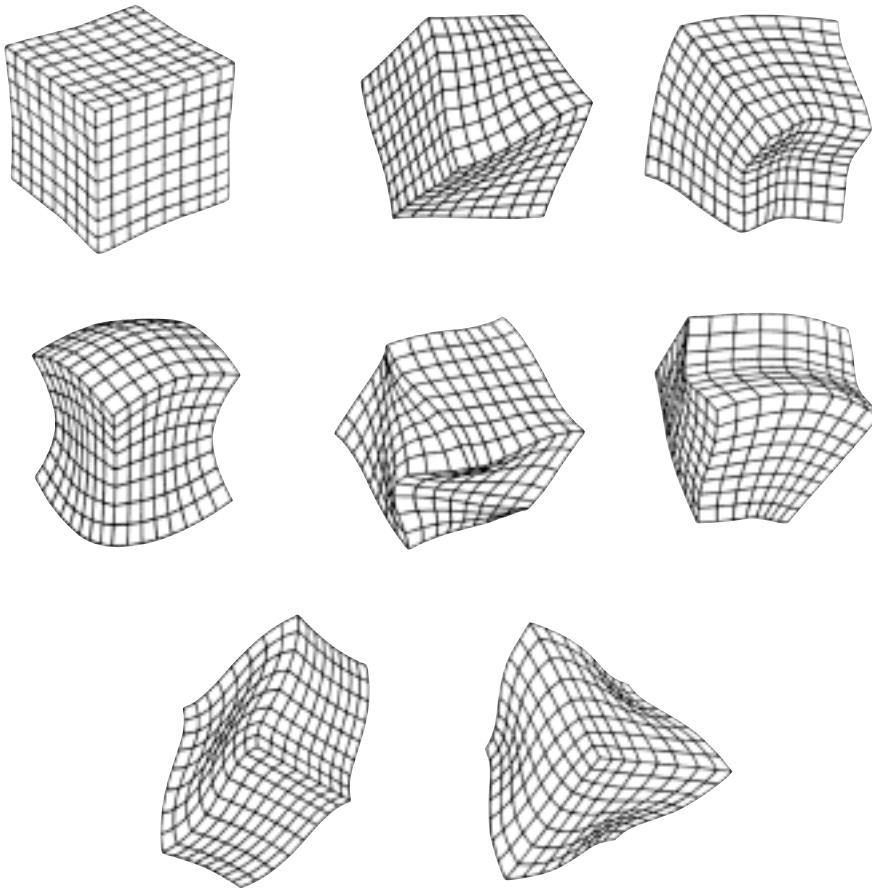


**Figure 10. Vibrational Modes of a Rectangular Parallelepiped**

There are eight types of normal vibrational modes for a crystalline sample of orthorhombic or higher symmetry shaped as a rectangular parallelepiped. The modes are either symmetric or anti-symmetric about three perpendicular planes. The lowest of each mode type is shown here.

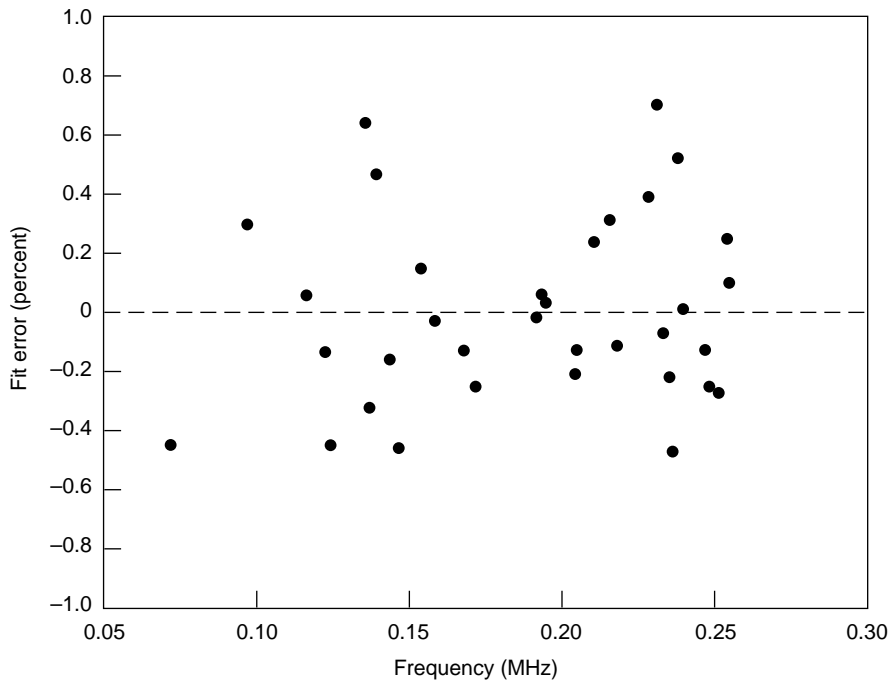


**Figure 11. Accuracy of RUS Measurements**

Shown here is the deviation between fitted and measured resonances on a typical polycrystalline plutonium sample. The experimental data are fed into a computer program that tries to find a set of elastic moduli consistent with the measured resonances, the sample dimensions, and the symmetry of the sample's crystal lattice. Each circle represents the difference between the observed and calculated resonances.

**Table II. Summary of Elastic-Moduli Measurements of Plutonium<sup>a</sup>**

Sample	$C_{11}$ (GPa)	Bulk (GPa)	Shear (GPa)
Polycrystal pure $\delta$ -Pu (703 K)	41.3	33.9	5.59
Polycrystal pure $\delta$ -Pu (655 K)	63.6	55.9	5.79
Single crystal $\delta$ -Pu 3.3 at. % Ga	51.4	29.9	16.1
Polycrystal $\delta$ -Pu 5.9 at. % Al	54.9	30.9	18.0
Polycrystal $\delta$ -Pu 2.1 at. % Al	40.3	19.1	15.9
Polycrystal $\delta$ -Pu 5.8 at. % Ga	65.1	37.1	21.0
Polycrystal $\delta$ -Pu 3.2 at. % Ga	64.4	37.7	20.0
Polycrystal $\delta$ -Pu 5.4 at. % Ga (aged)	50.0	27.0	17.2
Polycrystal $\delta$ -Pu 4.0 at. % Ga (aged)	58.4	34.3	18.1
Polycrystal $\delta$ -Pu 3.3 at. % Ga (new)	51.8	29.6	16.7
Polycrystal $\delta$ -Pu 3.3 at. % Ga (aged)	47.5	26.7	15.6
Polycrystal $\delta$ -Pu 2.2 at. % Ga (new)		30.3	
Cast $\alpha$ -Pu (laquer)	104.6	46.6	43.5
Cast $\alpha$ -Pu*	109.1	55.8	40.0
Cast $\alpha$ -Pu (DeCadenet)	109.0	54.5	40.9

<sup>a</sup> The measurements conducted by the authors of this article are in red. All measurements took place at ambient temperature except where noted.

a  $Q$  of 10,000 would enable us to see a change of about 1 ppm in stiffness, something we might expect to see in a few days if the temperature can be held stable to 0.005 kelvin, a perfectly feasible task. The second is a measurement that enables us to study the effects of aging on phase stability in real time. For example, if gallium-stabilized  $\delta$ -plutonium is cooled, it may become increasingly and measurably (by the RUS method) unstable, a feature exhibited by a very slow change in elastic moduli versus time. Such metastability is observed in many systems, including steel and precipitation-hardened aluminum (known as aircraft aluminum). To observe both radioactivity-induced changes and metastability will require a precisely temperature-controlled environment for the measurement. Such a system will leverage another critical set of measurements—the variation of mod-

uli with temperature.

One source of variation in the elastic properties of plutonium with temperature comes from changes in the phonon frequencies with vibrational amplitude—an important nonlinear effect, as is thermal expansion. Noting that plutonium has a very large thermal-expansion coefficient, other nonlinear effects are also expected to be unusually large. Their study will therefore be particularly revealing. Few temperature-dependent modulus measurements have been made so far, and there are no single-crystal data. The polycrystal work has been done on large samples that self-heat, and only one set of data appears on the gallium-stabilized alloy. The elastic moduli results of those measurements are substantially different from our recent results (the value for the 3.2 at. % gallium sample in Table II was taken from the temperature-dependence

study). Understanding the cause for those differences will be difficult and time-consuming but is badly needed. Our approach, especially considering the safety concerns, is to begin with measurements of the temperature variation of the elastic moduli around ambient temperature by using thermoelectrically cooled stages to vary temperature by 30 kelvins or so. Such a variation will enable us to determine the slope of the temperature dependence at ambient temperature to about 0.3 percent. This work is well under way, as we are tackling the much more difficult task of introducing furnaces and cryogenics into the RUS experimental area so that other phases can be studied. The results of this latter aspect of our work will be well worth our effort. ■

### Further Reading

- Eriksson, O. D., J. N. Becker, A. V. Balatsky, and J. M. Wills. 1999. *J. Alloys and Compounds* **287**: 1.
- Kmetko, E. A., and H. H. Hill. 1976. *J. Phys. F* **6** (6): 1025.
- Landau, L. D., and E. M. Lifshitz. 1980. *Statistical Physics*. Translated from Russian by J. B. Sykes and M. J. Kearsley. Oxford: Butterworth-Heinemann.
- Ledbetter, H. M., and R. L. Moment. 1975. *Acta Metall.* **24**: 891.
- Söderlind, P. 1998. *Adv. Phys.* **47**: 959.
- Wallace, D. C. 1998. *Phys. Rev. B* **58** (23): 890.



**Joe Baiardo** received his undergraduate degree in chemistry from Loyola University, Chicago, and his Ph.D. in chemical physics from the University of Florida. After completing postdoctoral work at the University of Florida and at Monsanto Corporate Research Laboratories, Joe became a staff member at Los Alamos. At first, he first worked on the Plutonium Molecular Laser Isotope Separation Project, primarily to develop methods for in situ time-resolved Fourier-transform optical spectroscopy of transient photochemical species. Subsequently, his efforts focused on development of an integrated spectroscopy system with unique capabilities for actinide surface science, applications of in situ Fourier-transform infrared surface characterization of actinide materials and acoustic-resonance spectroscopy of components, as well as resonant ultrasound measurements of elastic constants of plutonium alloys.



**Tim Darling** received his undergraduate degree and his Ph.D. from the University of Melbourne, Australia. Tim began his postdoctoral work in 1989 at the Los Alamos National Laboratory and is presently working as staff member on resonant ultrasound spectroscopy and electronic transport. For his work, Tim received a 1993 Distinguished Performance Award, the highest award granted by the Director of Los Alamos. His current interests are the fundamental connections between elastic moduli temperature variations and stability in solid-state systems and the role and sources of internal friction at low temperatures and high frequencies. Current experiments involve phase transformations in cubic systems, particularly on the formation and dynamics of martensitic phases.



**Albert Migliori** received his B.S. in physics from Carnegie-Mellon University and his Ph.D. in physics from the University of Illinois. He joined the Los Alamos National Laboratory as a Laboratory Director postdoctoral fellow and later became a staff member. He is codiscoverer of acoustic heat engines and a leading expert in the use of resonant ultrasound spectroscopy as a solid-state physics tool. For his work, Albert won R&D 100 awards in 1991 and 1994; a Federal Laboratory Consortium Award for Excellence in Technology Transfer in 1993; and a Los Alamos National Laboratory Distinguished Performance Award in 1994. Albert is a Fellow of the American Physical Society and the Los Alamos National Laboratory.